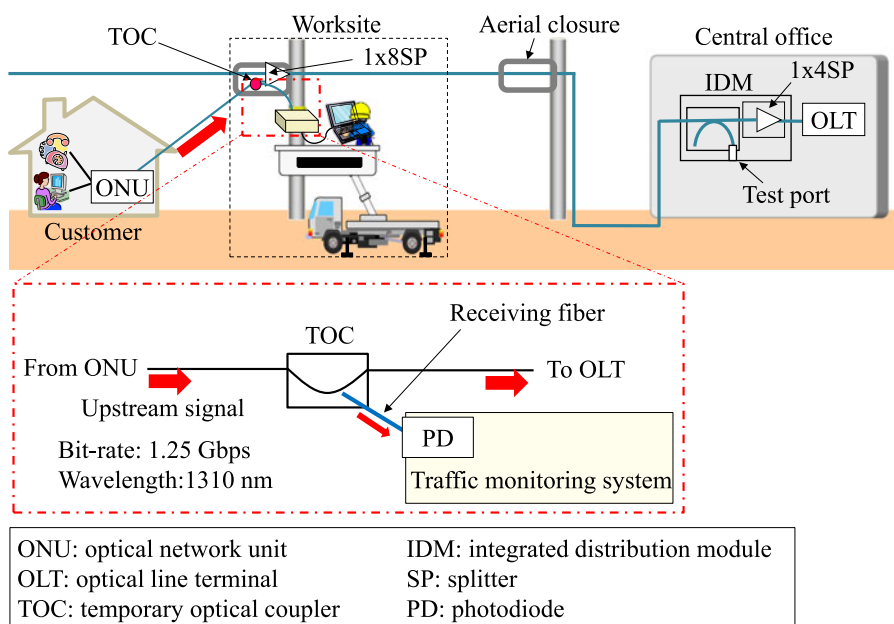


Design of a Temporary Optical Coupler Using Fiber Bending for Traffic Monitoring

Volume 9, Number 6, December 2017


Takui Uematsu
Hidenobu Hirota
Tomohiro Kawano
Takanori Kiyokura
Tetsuya Manabe



DOI: 10.1109/JPHOT.2017.2762662

1943-0655 © 2017 IEEE

Design of a Temporary Optical Coupler Using Fiber Bending for Traffic Monitoring

Takui Uematsu , Hidenobu Hirota, Tomohiro Kawano,
Takanori Kiyokura, and Tetsuya Manabe

Access Network Service Systems Laboratories, NTT Corporation, Tsukuba
305-0805, Japan

DOI:10.1109/JPHOT.2017.2762662

1943-0655 © 2017 IEEE. Translations and content mining are permitted for academic research only.
Personal use is also permitted, but republication/redistribution requires IEEE permission.
See http://www.ieee.org/publications_standards/publications/rights/index.html for more information.

Manuscript received August 31, 2017; revised October 2, 2017; accepted October 10, 2017. Date of publication October 13, 2017; date of current version November 2, 2017. Corresponding author: Takui Uematsu (e-mail: uematsu.takui@lab.ntt.co.jp).

Abstract: We design a temporary optical coupler that extracts 1.25-Gbps optical signals for traffic monitoring. The temporary optical coupler employs a fiber bending technique that uses a receiving fiber to receive leaked signal light from a bent fiber. We optimize the bending condition and the receiving fiber to obtain a high extraction efficiency while keeping the bending loss below 2 dB. We also measure the bit error rates for the 1.25-Gbps signals and reveal that our temporary optical coupler extracts the 1.25-Gbps optical signals without any deterioration in signal quality. Finally, we confirm experimentally that we achieved traffic monitoring using a traffic monitoring system and our temporary optical coupler in a fiber-to-the-home access network system based on a gigabit Ethernet passive optical network.

Index Terms: Optical fiber applications, optical fiber couplers, optical fiber devices.

1. Introduction

Broadband access network services via optical fibers are widely used throughout the world. Passive optical networks (PONs) such as gigabit-PON (G-PON) [1] and gigabit Ethernet PON (GE-PON) [2] are mainly used to provide fiber-to-the-home (FTTH) services. The number of optical fiber cables has increased along with the rapid increase in the number of FTTH subscribers. Thus it is important to undertake fiber cable construction and maintenance efficiently.

Non-destructive fiber bending techniques have been proposed in order to realize efficient construction and maintenance [3]–[11]. With the technique, leaked light is used to extract signals from the bent fiber. The technique also enables us to insert light from outside into a bent fiber [6]–[10]. In other words, the technique can realize an optical coupler temporarily at any point without the need to cut the fiber. So temporary optical couplers (TOCs) employing the technique are used for fiber identification, fiber communications, fiber monitoring, temporary test instrument connection, and detour route formation without cutting in-service fibers.

Fig. 1 shows an application of the TOC to a typical FTTH access network based on a GE-PON. Optical network units (ONUs) are installed on customer premises and optical line terminals (OLTs) are installed in a central office for FTTH access network services. A traffic monitoring system (TMS) receives upstream optical signals that are transmitted from the ONUs to the OLT, and it observes the link status between the OLT and the ONUs and monitors the services being used by each ONU [12], [13]. With the conventional method, the TMS is connected to a fiber test port, which is used

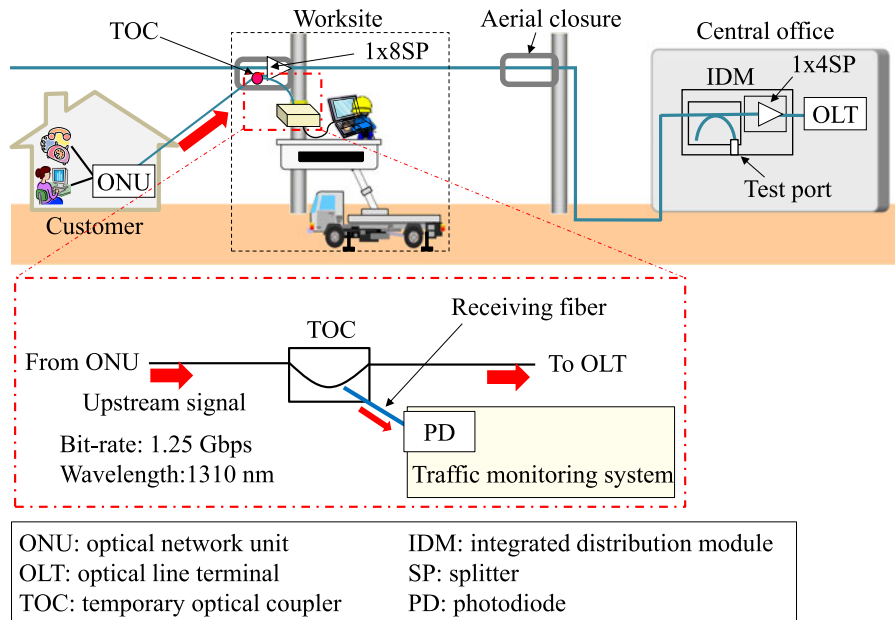


Fig. 1. Application of the temporary optical coupler to a typical FTTH access network based on GE-PON.

TABLE 1
Requirements for the TOC

No.	Items	Requirements
1	Bending loss (Insertion loss) L	≤ 2 dB over communication wavelength bands [11]
2	Extraction efficiency η	≥ -18.5 dB at a wavelength of 1310 nm

for testing with an optical time domain reflectometer installed in an integrated distribution module (IDM) in a central office. On the other hand, with our proposed method, the TMS is connected to the receiving fiber of the TOC, and it receives the upstream optical signals that are extracted by the TOC. Our proposed method enables us to observe the link status and monitor the services being used by each ONU at a worksite immediately, for example in optical aerial closures. It leads to the more efficient construction and maintenance of fiber cables, and higher quality FTTH access network services. Table 1 shows the requirements for the TOC to realize our proposed method. First, the bending loss of the TOC should be suppressed to no more than 2 dB over communication wavelength bands (see Appendix I in [11]) for traffic monitoring by the TMS. This is because a high bending loss will cause deterioration in the signal quality of transmission systems and at worst service interruption, and then the TMS will not monitor the ONUs because they do not output the upstream optical signals to the OLT. Second, the requirement as regards the extraction efficiency is derived from the following equation,

$$P_{ONU} - L_{8SP} + \eta \geq R_{PD} \quad (1)$$

where P_{ONU} is the output power from an ONU, L_{8SP} is the insertion loss of a 1×8 splitter (SP), R_{PD} is the receiving sensitivity of the photodiode (PD) in the TMS, and η is the extraction efficiency of the TOC. P_{ONU} is set at -1 dBm because the minimum ONU output power is -1 dBm for 1000BASE-PX10 (for GE-PON) [2]. L_{8SP} is set at 10.5 dB because the insertion loss of the 1×8 SP in an

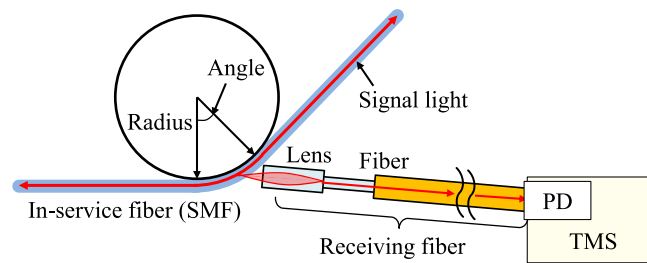


Fig. 2. Basic concept of the TOC with the TMS.

optical aerial closure is no more than 10.5 dB [14]. R_{PD} is set at -30 dBm because an avalanche PD (APD) with a receiving sensitivity of no more than -30 dBm is available [15]. Therefore η derived from (1) is no less than -18.5 dB.

With the conventional methods proposed in [7]–[10], a receiving fiber and/or lens are closely placed to capture the leakage light instead of the PD. The receiving fiber is standard single-mode fiber (SMF), and the lens is placed between the bent fiber and the SMF to focus the leakage light into the core of the SMF. An extraction efficiency of -20 dB is achieved at a wavelength of 1310 nm for a clip-on coupler [7]. And an extraction efficiency of -17.8 dB is achieved at a wavelength of 1310 nm for [10]. However, the bending losses of these TOCs [7]–[10] are high due to tight bending because a higher bending loss generally increases the extraction efficiency. For example, the typical insertion losses are 7 dB for [7] and over 15 dB for [10], respectively, at a wavelength of 1310 nm. These insertion losses do not meet the bending loss requirement shown in Table 1.

Optical fiber identifiers have been widely used as conventional tools for identifying a specific fiber and thus avoiding incorrect cutting and connection at a worksite [3]–[5]. These fiber identifiers have a bending loss of less than 2 dB over communication wavelength bands to maintain the transmission quality [11]. In these identifiers, a large-area PD (diameter of a few millimeters) is positioned so that it receives sufficient diffused leakage light from the bent fiber because an identification light with a low frequency (e.g., 270 Hz) is input into the fiber in question [11]. On the other hand, a small-area PD is needed to extract 1.25 Gbps signals for a GE-PON; for example, the active-area diameter of a PD is typically about $55 \mu\text{m}$ ($75 \mu\text{m}$ at most) for a GE-PON [16]. In addition, the PD in the TMS cannot be placed close enough to the bent fiber to receive the diffused leakage light because of the limitation imposed by the size ($170 \times 90 \times 270$ mm) and the weight (about 5.1 kg) of the TMS. Thus the TOC should be separated from the TMS and its receiving fiber connected to the TMS port.

In this paper, we design a TOC that extracts 1.25 Gbps optical signals for traffic monitoring. First, we design the bending condition needed to obtain a high extraction efficiency while keeping the bending loss below 2 dB. Second, we design the receiving fiber to obtain a high extraction efficiency to meet requirement 2 shown in Table 1. We utilize a multi-mode fiber (MMF) with a gradient index (GRIN) lens implemented at its tip to focus the leakage light on the core of the MMF. We measure bit-error rates (BER) for 1.25 Gbps signals and reveal that our TOC extracts the 1.25 Gbps optical signals without any deterioration in signal quality. Third, we reveal the optical properties of our TOC. Finally, we confirm experimentally that we achieved traffic monitoring using the TMS and our TOC in an FTTH access network system based on a GE-PON.

2. Basic Concept

Fig. 2 shows the basic concept of the TOC with the TMS. Leakage light from a bent fiber with a bending radius R and a bending angle θ are received by a receiving fiber. The radius and angle are set so that the bending loss is no more than 2 dB over the communication wavelength bands to meet requirement 1. The receiving fiber consists of a fiber and a GRIN lens, which focuses the leakage light on the core of the receiving fiber. The GRIN lens is spliced to the fiber. The diameter of the GRIN lens should be as small as possible to allow the lens to access the bent fiber. The signal

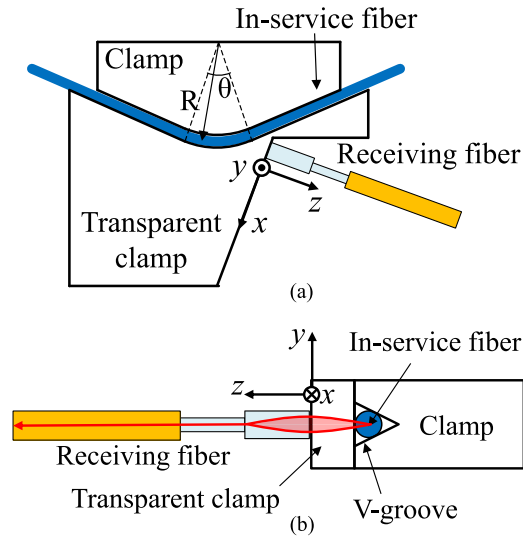


Fig. 3. Structure of the TOC. (a) Top view. (b) Side view.

light received by the receiving fiber is detected by the PD in the TMS. The extraction efficiency from the bent fiber to the receiving fiber must meet requirement 2 because the power of the received signal light must overcome the receiving sensitivity of the PD in the TMS.

3. Design

Fig. 3 shows the structure of the TOC. We use a convex clamp with a V-groove and a concave clamp made of optically transparent plastic to bend the fiber with the correct bending radius R and angle θ . The refractive index of the transparent plastic is higher than that of the fiber coating to avoid any reflection of the leakage light at the boundary between the bent fiber and the transparent clamp. The V-groove is used to keep the fiber with a coating diameter of $250 \mu\text{m}$ in the correct position without any stress. The receiving fiber is placed at the point where it captures the most leakage light and is glued onto the transparent clamp with UV curable resin. The advantage of these methods is that they receive a lot of leakage light and guide it into the PD in the TMS because the receiving fiber or the lens can be placed close to the bent fiber. To meet the requirements in Table 1, we need to choose a bending condition and a receiving fiber to obtain a high extraction efficiency while keeping the bending loss at no more than 2 dB. We optimize the bending condition and the receiving fiber below.

3.1 Design of Bending Radius and Angle

First, we decided the bending radius R . Fig. 4 shows the leakage light being received by the receiving fiber from a bent fiber. P_{in} and P_{out} are the input and output powers of the bent fiber, respectively. The power of the leakage light P_{leak} is given by

$$P_{leak} = P_{in} - P_{out} = P_{in} (1 - e^{-2\alpha R\theta}) \quad (2)$$

where α is the bending loss per unit length [17]. The power of the leakage light that can be received by the GRIN lens of the receiving fiber P_{rec} is directly proportional to the receiving efficiency. The receiving power P_{rec} is expressed as

$$P_{rec} = P_{in} (1 - e^{-2\alpha R\Delta\theta}) \quad (3)$$

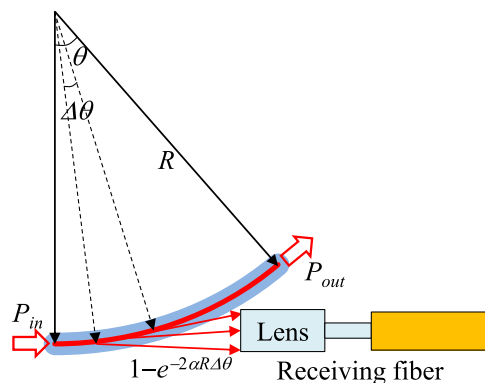


Fig. 4. Image of leakage light being received from a bent fiber by the receiving fiber.

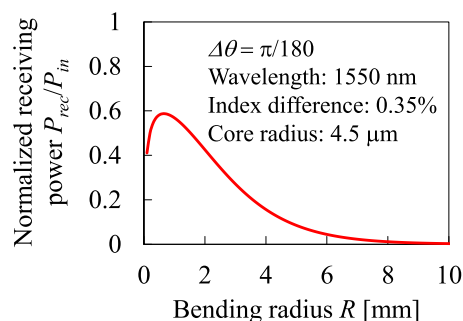


Fig. 5. Normalized receiving power P_{rec}/P_{in} as a function of bending radius R . The parameters used are inset in the figure.

where $\Delta\theta$ is the angle of the leakage region the leakage light from which is received by the receiving fiber. Fig. 5 shows the normalized receiving power P_{rec}/P_{in} as a function of the bending radius R when $\theta = \pi/180$. A smaller radius makes the receiving power higher when R is above 0.6 mm. Therefore, a smaller radius would achieve a high extraction efficiency.

On the other hand, mechanical reliability should be considered because tight bending may result in fiber failure. Fig. 6 shows the fiber failure probability as a function of the bending radius calculated based on the Weibull distribution [18]. In the calculation, the bending angle θ is $\pi/2$, the bending times are set at 1 day, 1 year, and 20 years and the other parameters have typical values [18], [19]. The fiber strength distribution is composed of intrinsic and extrinsic flaw distributions with different slope parameters. Fig. 6 shows that the fiber failure probability increases abruptly when R becomes smaller than 2 mm and the bending time is 20 years. Thus we chose $R = 2$ mm to achieve both a high extraction efficiency and high reliability.

Next, we decided the bending angle θ . Fig. 7 shows the estimated maximum extraction efficiency η_{max} as a function of bending loss L . η_{max} is the normalized power of the leaked light from the bent fiber and is given by

$$\eta_{max} = 10 \log_{10} \left(1 - 10^{-\frac{L}{10}} \right) \quad (4)$$

η_{max} , namely Fig. 7 reveals that the extraction efficiency increases as the bending loss increases. Fig. 8 shows experimental results for bending loss L at a wavelength of 1550 nm with different bending angles θ and $R = 2$ mm. In the experiment, we used a convex clamp with a V-groove and the concave transparent clamp shown in Fig. 3 to bend the fibers. The bent fiber was compatible with ITU-T G.652 [20]. The coating diameter was 250 μm , the mode field diameter was 9.4 μm at

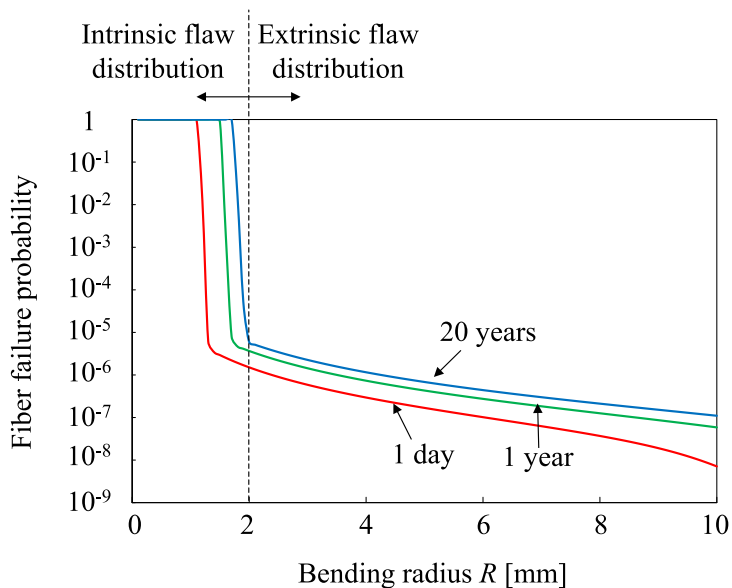


Fig. 6. Fiber failure probability as a function of bending radius R calculated based on the Weibull distribution. The bending angle θ is $\pi/2$, the bending times are 1 day, 1 year, and 20 years, and the other parameters are set at typical values [18], [19].

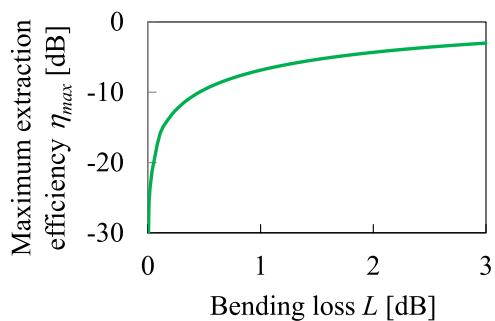


Fig. 7. Estimated maximum extraction efficiency η_{max} as a function of bending loss L . η_{max} is calculated with (4).

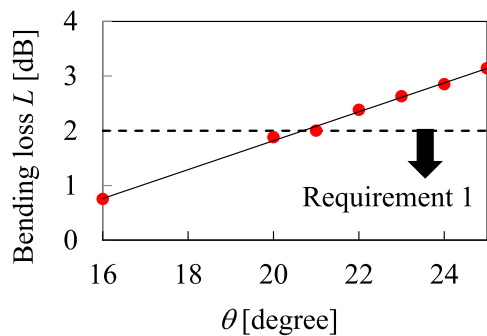


Fig. 8. Bending loss L at a wavelength of 1550 nm with different bending angles for $R = 2$ mm.

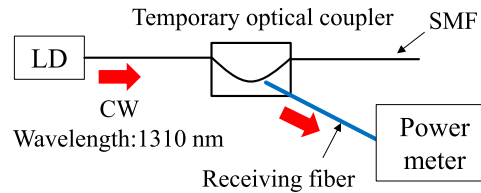


Fig. 9. Experimental setup for measuring the extraction efficiency η_C . The receiving fibers used are listed in Table 1.

a wavelength of 1310 nm, and the cut-off wavelength was 1260 nm. Fig. 8 shows that the bending loss decreased as the bending angle became more acute, namely the length of the bend became shorter. We selected $\theta = 20^\circ$ to obtain a bending loss of less than 2 dB and a high extraction efficiency.

3.2 Design of Receiving Fiber

To capture the diffused leakage light from the bent fiber, we used an MMF with a large diameter core as the receiving fiber. A GRIN lens was employed at the tip of the MMF to focus the captured leakage light on the core of the MMF. The extraction efficiency η is given by

$$\eta = \eta_C - \delta \quad (5)$$

$$\eta_C = \eta_{\max} - L_C \quad (6)$$

where η_C is the extraction efficiency of the receiving fiber and δ is the BER power penalty caused by the transmission loss and modal dispersion in the MMF, and the coupling loss L_{PD} between the MMF and the PD in the TMS. L_C is the coupling loss between the bent fiber and the receiving fiber, including the losses in the fiber coating and the transparent clamp. L_C will decrease as the core diameter increases, which means that η_C will be improved. On the other hand, the PD in the TMS has a small active-area diameter for high-bit-rate signals, for example, 55 μm for 1.25 and 2.5 Gbps signals [16] and 22 μm for 10 Gbps signals [21]. A larger core diameter would result in a higher coupling loss L_{PD} . Therefore we should choose an appropriate core diameter so that η is maximized.

We measured the extraction efficiency η_C using the experimental setup shown in Fig. 9. The receiving fibers we used are listed in Table 2. The MMFs were about 2 m long to reduce the deterioration in signal quality caused by mode dispersion in the MMF and to connect with the TMS that is placed on a work table. The sample fibers were compatible with ITU-T G.652 [20]. The coating diameter was 250 μm and the cut-off wavelength was 1260 nm. We set the GRIN lens diameters at less than 250 μm to reduce the optical transmission loss of the transparent clamp by placing it close to the bent fiber. The beam waist (BW) diameters were designed to be as wide as possible to capture a lot of leakage light. The BW distances were designed to be 500-1000 μm because we estimated that the distance between the GRIN lens and the leakage point of the bent fiber is 500-1000 μm . Fig. 10 shows the experimental results we obtained for the extraction efficiency η_C at a wavelength of 1310 nm. A higher η_C was obtained when the core diameter of the receiving fiber was larger, namely the BW diameter was larger. It can be seen that η_C converged to about -15 dB when the core diameter was larger.

Next, we investigated the BER power penalty caused by using the MMF. We measured the BER with the experimental setup shown in Fig. 11. We used a commercial duplex small form-factor pluggable (SFP) transceiver, which complies with Gigabit Ethernet as specified in IEEE Std. 802.3 [2]. The active-area diameter of the PD in the SFP equals that in the TMS. The receiving fibers listed in Table 2 were about 2 m long to suppress the mode dispersion and were directly connected to the PD of the SFP. The BER of a back-to-back transmission was also measured via an SMF without the TOC. Fig. 12 shows the BER of the TOC at a wavelength of 1310 nm. The input power

TABLE 2
Parameters of Receiving Fibers

Name	SMF	GI50	GI62.5	SI105
Index profile	SI	GI	GI	SI
Core diameter [μm]	8.2	50	62.5	105
Cladding diameter [μm]	125	125	125	125
Numerical aperture	0.14	0.2	0.275	0.2
Lens diameter [μm]	125	246	250	250
Lens length [μm]	1696	1119	1206	2247
Beam waist diameter [μm]	25*	148**	169**	223**
Beam waist distance [μm]	1071*	692**	787**	528**

*wavelength: 1310 nm, **wavelength: 850 nm.
The GRIN lenses are optimized so that the beam waist diameter is maximized at a distance of 500–1000 μm .

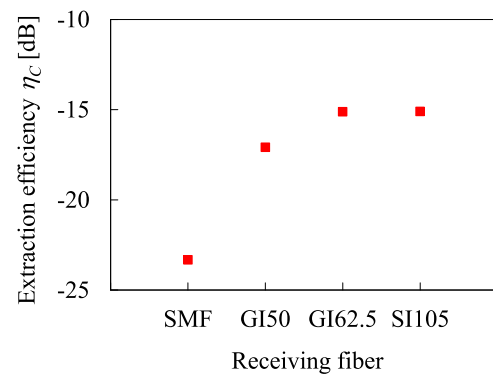


Fig. 10. Experimental results for extraction efficiency η_c at a wavelength of 1310 nm. The receiving fibers are as listed in Table 2.

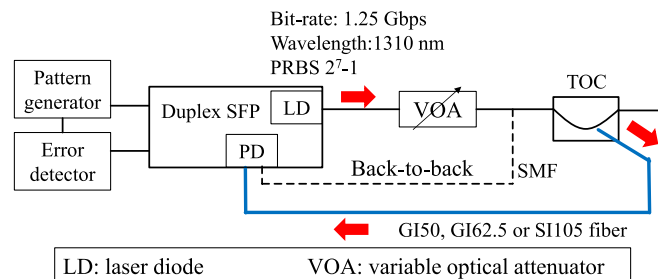


Fig. 11. Experimental setup for BER measurement. The receiving fibers are about 2 m long and are directly connected to the PD of a commercial duplex small form-factor pluggable (SFP) transceiver that complies with Gigabit Ethernet as specified in IEEE Std. 802.3. The active-area diameter of the PD in the SFP almost equals that in the TMS.

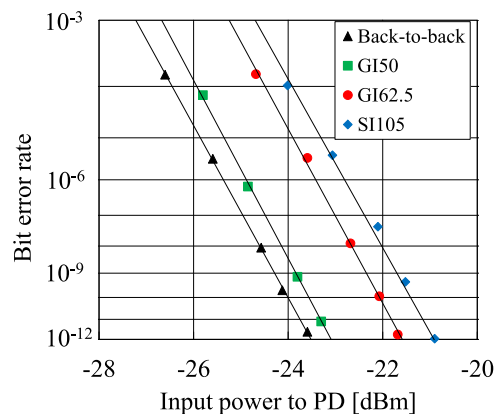


Fig. 12. BER of the TOC at a wavelength of 1310 nm. Input power to PD means the power of the signal light input from the MMF into the PD. The receiving fibers are listed in Table 2.

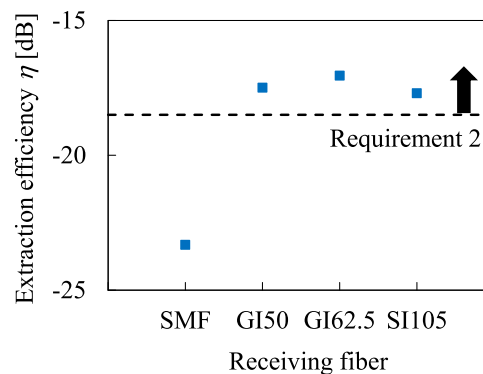


Fig. 13. Extraction efficiency η derived from Fig. 10, Fig. 12, and (5) at a wavelength of 1310 nm. The receiving fibers listed in Table 2 are used.

to the PD in Fig. 12 means the power of the signal light input from the MMF to the PD. The power penalty compared with the back-to-back transmission became higher as the core diameter of the receiving fiber increased. The power penalties are caused by the coupling loss L_{PD} and the modal dispersion in the MMF, because the measured coupling losses were 0.5 and 1.25 dB for GI50 and GI62.5, respectively. Fig. 13 shows the extraction efficiency η at a wavelength of 1310 nm. η is derived from the receiving efficiency η_C shown in Fig. 10, the measured power penalty in Fig. 12, and eq. (5). The highest extraction efficiency η was obtained when the receiving fiber was GI62.5. Moreover, requirement 2 is met by using GI50, GI62.5, or SI105 as the receiving fiber.

4. Properties

In this section, we investigate the properties of the TOC designed in section 3. The bending radius and angle are 2 mm and 20° , respectively. The receiving fiber is GI62.5 as shown in Table 2. The sample fibers are compatible with ITU-T G.652 [20]. The coating diameter is $250 \mu\text{m}$ and the cut-off wavelength is 1260 nm. Fig. 14 shows the measured bending loss of the TOC at wavelengths of 1310, 1490, and 1550 nm. The bending loss is less than 2 dB over the communication wavelength bands, which meets the requirement 1. Fig. 15 shows the measured extraction efficiency η_C and the calculated receiving efficiency η_{max} at wavelengths of 1310, 1490, and 1550 nm. η_{max} is derived from (4) by using the bending loss shown in Fig. 14. An η_C value of more than -15.2 dB can be obtained over the communication wavelength bands. The wavelength dependence of η_C is similar

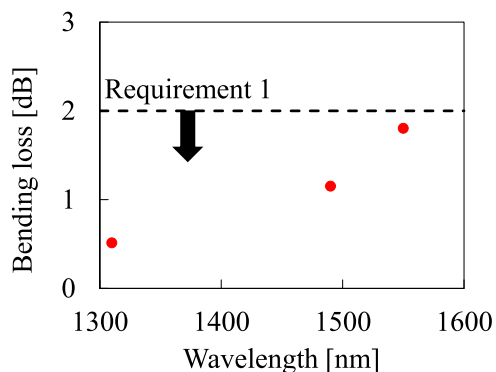


Fig. 14. Measured bending loss of the TOC at wavelengths of 1310, 1490, and 1550 nm.

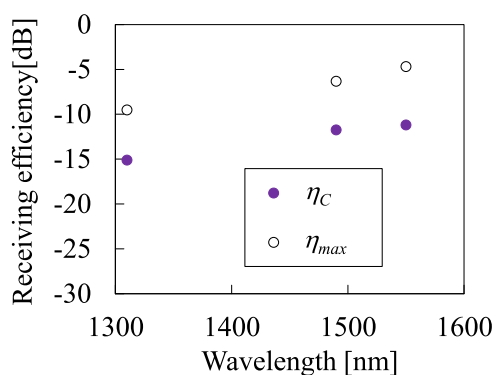


Fig. 15. Extraction efficiency η_C and η_{max} of the temporary optical coupler at wavelengths of 1310, 1490, and 1550 nm. η_{max} is derived from (4) by using the bending loss in Fig. 14.

to that of η_{max} derived from the bending loss. Thus the wavelength dependence of η_C would result from that of the bending loss.

We also measured the position tolerance in order to consider the variation in the extraction efficiency when the bent fiber is not held in the correct position due to variations in the structure of the bent fiber and mechanical deviations of the clamps. Fig. 16 shows the experimental position tolerance results we obtained when the receiving fiber moved in transverse directions (a) x, (b) y, and a propagation direction (c) z as shown in Fig. 3. A higher tolerance was obtained compared with the SMF receiving fiber by expanding the BW diameter of the receiving fiber using GI62.5. Even when there was a misalignment of 50 μm , the decrease in the extraction efficiency was below 1 dB and the TOC met requirement 2. This shows that we achieved ease of fabrication and a stable extraction efficiency.

5. Application

In this section, we confirm experimentally that we achieved traffic monitoring by using the TMS and our TOC in an FTTH access network system based on a GE-PON as shown in Fig. 1. Fig. 17 shows our experimental setup for confirming the feasibility of traffic monitoring. The TOC was installed at monitoring point 1 or 2. We verified that the TMS could observe the link status between the ONU and the OLT when the power of the upstream signal from the ONU was reduced by the VOA. The TMS observed the link status when the attenuation was below 12.5 dB for monitoring point 1 and below 3 dB for point 2.

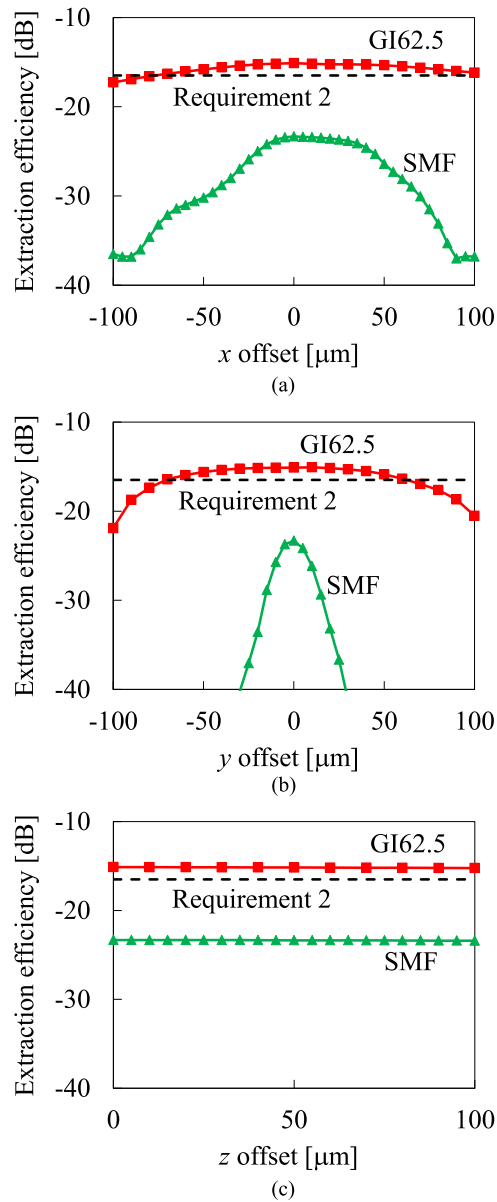


Fig. 16. Experimental results for position tolerance when the receiving fiber moves in the transverse directions (a) x, (b) y, and the propagation direction (c) z. Coordinate axes are shown in Fig. 3. Dashed lines show requirement 2.

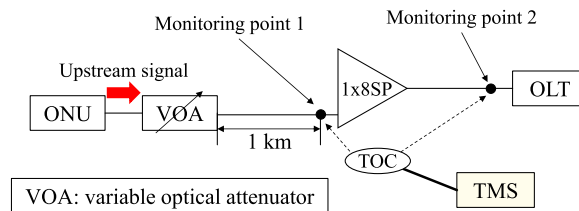


Fig. 17. Experimental setup for confirming the feasibility of traffic monitoring with the TMS and the TOC. The TOC was temporarily installed at the monitoring point 1 or point 2.

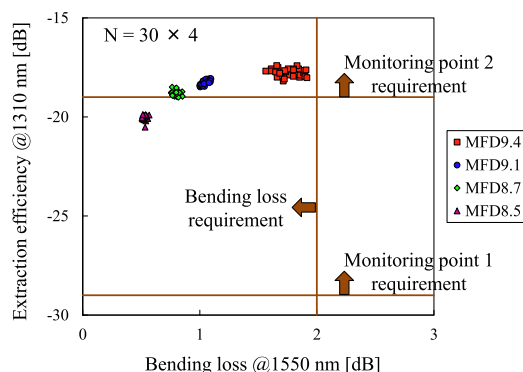


Fig. 18. Extraction efficiency versus bending loss of our TOC. The sample fibers were compatible with ITU-T G.652 [20] and ITU-T G.657 [22]. We performed 30 measurements for each of four fibers that had MFDs of 8.5, 8.7, 9.1, and 9.4 μm , respectively.

In an FTTH access network based on a PON, 0.25-mm-diameter acrylate coated fibers are mainly installed at the connection points in aerial closures for fusion splicing. Traffic monitoring with our TOC will be applied to these 0.25-mm-diameter coated fibers. The fibers installed in aerial closures are compatible with ITU-T G.652 (minimum bending radius = 30 mm) [20] or ITU-T G.657 (minimum bending radius = 15 mm) [22]. So we target these fibers in this paper. Fig. 18 shows the extraction efficiency versus the bending loss of our TOC. The sample fibers were compatible with ITU-T G.652 and ITU-T G.657. We measured the extraction efficiency and bending loss 30 times each for four fibers that had mode field diameters (MFD) of 8.5, 8.7, 9.1, and 9.4 μm , respectively. The bending loss and the extraction efficiency increased as the MFD increased. The measured results met the bending loss and extraction efficiency requirements at point 1. This showed that our TOC realized traffic monitoring in aerial closures below the 1 x 8 SP. However, the results for the fiber with an MFD of 8.5 μm did not meet the extraction efficiency requirement at point 2 in Fig. 17. We must increase the bending loss of the fibers with a small MFD or the extraction efficiency for monitoring at point 2.

6. Conclusion

We designed a TOC that extracts 1.25 Gbps optical signals for traffic monitoring. First, we optimized the bending condition to obtain a high extraction efficiency while keeping the bending loss below 2 dB. Second, we chose a receiving fiber that provided a high extraction efficiency to meet requirement 2 shown in Table 1. An extraction efficiency of -17 dB was obtained that met requirement 2 by utilizing an MMF with a GRIN lens. We also measured the BER for 1.25 Gbps signals and revealed that our TOC extracted 1.25 Gbps optical signals without any deterioration in signal quality. Third, we investigated the optical properties of our TOC and revealed that it achieved ease of fabrication and a stable extraction efficiency. Finally, we confirmed that we achieved traffic monitoring using the TMS and our TOC in an FTTH access network system based on a PON. Our proposed method enabled us to observe temporarily the link status and monitor services being used by each ONU at any point without cutting an in-service fiber. This approach will lead to the more efficient construction and maintenance of fiber cables, and higher quality FTTH access network services.

References

- [1] *Gigabit-Capable Passive Optical Networks (GPON): General Characteristics*, ITU-T Rec. G. 984, Mar. 2008.
- [2] *IEEE Standard for Information Technology—Telecommunications and Information Exchange Between Systems—Local and Metropolitan Area Networks—Specific Requirements*, IEEE 802.3ah, Sep. 2004.

- [3] M. D. Feuer and V. A. Vaishampayan, "Clip-on fiber identifier using digital lightpath labels," *Proc. SPIE*, vol. 7632, 2009, Art. no. 763220.
- [4] T. Matsui, K. Nakajima, K. Toge, T. Kurashima, and M. Tsubokawa, "Fiber identification technique based on mechanically-induced long-period grating for bending-loss insensitive fibers," *J. Lightw. Technol.*, vol. 28, no. 24, pp. 3556–3561, Dec. 2010.
- [5] K. Matsuoka, S. Niimi, M. Miyamoto, and H. Sugawara, "New optical fiber identifier," in *Proc. 64th Int. Cable Connectivity Symp.*, Oct. 2015, pp. 704–708.
- [6] M. Shimizu, S. Takashima, and H. Kobayashi, "Identification system for optical fiber transmission operation lines with local-light injection and detection coupling system," *J. Lightw. Technol.*, vol. 10, no. 5, pp. 686–692, May 1992.
- [7] Go4Fiber, "Passive fiber clip-on coupler," 2017. [Online]. Available: <https://www.go4fiber.com/spec/PFC%201000.pdf>
- [8] H. Hirota *et al.*, "Fiber identification below an optical splitter with a test light injection tool," *J. Lightw. Technol.*, vol. 33, no. 13, pp. 2751–2757, Jul. 2015.
- [9] T. Manabe *et al.*, "Temporary optical coupler and dynamic delay adjustment technologies for optical cable re-routing operation support systems," in *Proc. 64th Int. Cable Connectivity Symp.*, Oct. 2015, pp. 709–714.
- [10] H. Hirota *et al.*, "Optical cable changeover tool with light injection and detection technology," *J. Lightw. Technol.*, vol. 34, no. 14, pp. 3379–3388, Jul. 2016.
- [11] *Optical Fibre Identification for the Maintenance of Optical Access Networks*, ITU-T Rec. L.85, Jul. 2010.
- [12] T. Isomura, S. Shimazu, Y. Fujimoto, and H. Kataoka, "Traffic monitoring system for fiber-to-the-home engineering work," *NTT Tech. Rev.*, vol. 7, no. 8, pp. 1–5, Aug. 2009. [Online]. Available: <https://www.ntt-review.jp/archive/ntttechnical.php?contents=ntr200908le2.html>
- [13] W. Kuratani, M. Shimpō, K. Toge, and S. Sako, "Optical cable network reconfiguration by employing ONU upstream signal monitoring technique for effective maintenance in optical access network," in *Proc. 62nd Int. Cable Connectivity Symp.*, Nov. 2013, pp. 21–25. [Online]. Available: http://www.iwcs.org/56333-iwcs-2013-a-1.1581598/t-001-1.1582469/f-002-1.1582470/2-2-1.1582480/2-2-1.1582481#tab_0=0
- [14] *Transmission Characteristics of Optical Components and Subsystems*, ITU-T Rec. G. 671, Jan. 2009.
- [15] Go!foton, "InGaAs Avalanche Photodiode (APD) 1.25Gbps BM APD-TIA," 2017. [Online]. Available: <http://gofoton.wpengine.netdna-cdn.com/wp-content/uploads/2014/10/PDAF0055TOL-T20-Rev2.pdf>
- [16] Go!foton, "InGaAs Avalanche Photodiode," 2017. [Online]. Available: <https://welcome.gofoton.com/wp-content/uploads/2014/10/PDAF0055C.pdf>
- [17] D. Marcuse, "Curvature loss formula for optical fibers," *J. Opt. Soc. Amer.*, vol. 66, no. 3, pp. 216–220, Mar. 1976.
- [18] W. Griffioen, W. Greven, J. Jonker, S. Zandberg, G. Kuyt, and B. Overton, "Reliability of bend insensitive fibers," in *Proc. 58th Int. Cable Connectivity Symp.*, Nov. 2009, pp. 251–257.
- [19] M. Tachikura, Y. Kurosawa, and Y. Namekawa, "Improved theoretical estimation of mechanical reliability of optical fibers," *Proc. SPIE*, vol. 5623, pp. 622–629, Jan. 2005.
- [20] *Characteristics of a Single-Mode Optical Fibre and Cable*, ITU-T Rec. G. 652, Nov. 2016.
- [21] Go!foton, "InGaAs Avalanche Photodiode (APD) 10 Gbps(Chip)," 2017. [Online]. Available: https://welcome.gofoton.com/wp-content/uploads/2013/06/APD10_PDAB0022C_rev1-GF.pdf
- [22] *Characteristics of a Bending-Loss Insensitive Single-Mode Optical Fibre and Cable*, ITU-T Rec. G. 657, Nov. 2016.